Observations of particle formation and growth in a mountainous forest region in central Europe

A. Held,[1,2] A. Nowak,[3] W. Birmili,[3] A. Wiedensohler,[3] R. Forkel,[4] and O. Klemm[1,2]

Received 13 August 2004; revised 22 September 2004; accepted 4 October 2004; published 7 December 2004.

[1] In the summers of 2001 and 2002, particle formation and growth were observed at a forest ecosystem research site in the "Fichtelgebirge" mountain range in NE Bavaria, Germany. Atmospheric nucleation events, identified through detailed analysis of the time evolution of submicron particle size distributions, differed considerably from nonevent days with respect to ultrafine particle concentrations and meteorological parameters. Particle diameter growth rates, as quantified through the geometric mean diameter development of the 3–60 nm particle fraction, ranged from 2.2 to 5.7 nm h^{-1}. While H_2SO_4 concentrations typically explained less than 10% of the observed growth rates, a significant fraction of particle growth may be explained through condensation of organic vapors from α-pinene oxidation. On several days, cocondensation of H_2SO_4 and α-pinene oxidation products was sufficient to fully explain the observed growth dynamics. While BVOC emissions from the tree vegetation may contribute to particle formation, the forest also acts as an effective sink for particles. This is reflected in the dominance of particle deposition to the forest over emission, with the strongest deposition fluxes occurring during particle formation events. *INDEX TERMS:* 0305 Atmospheric Composition and Structure: Aerosols and particles (0345, 4801); 0315 Atmospheric Composition and Structure: Biosphere/atmosphere interactions; 0322 Atmospheric Composition and Structure: Constituent sources and sinks; 0365 Atmospheric Composition and Structure: Troposphere—composition and chemistry; *KEYWORDS:* particle growth, particle dynamics, forest

Citation: Held, A., A. Nowak, W. Birmili, A. Wiedensohler, R. Forkel, and O. Klemm (2004), Observations of particle formation and growth in a mountainous forest region in central Europe, *J. Geophys. Res.*, *109*, D23204, doi:10.1029/2004JD005346.

1. Introduction

[2] Aerosol particles are in the focus of current atmospheric research activities due to their relevance for the radiation budget, due to their chemical reactivity, and for hygienic issues, amongst others. While many mechanisms of direct particle emission into the atmosphere are well understood, the secondary formation of particulate matter in the atmosphere through gas-to-particle conversion processes still has to be elucidated. Chemical species occurring in both the condensed and gaseous forms are distributed between the gas and particle phases according to their thermodynamical equilibrium [e.g., *Wexler and Seinfeld*, 1990]. Deviations from this equilibrium may occur as a result of chemical reactions or temperature variations, leading to supersaturation with respect to the saturation pressure of the considered vapor. The equilibrium is reestablished through gas-to-particle conversion of the compound by (1) homogeneous nucleation resulting in formation of new particles, or (2) heterogeneous nucleation, i.e., condensation of low-volatile vapors on existing particle surfaces [e.g., *Seinfeld and Pandis*, 1998; *Friedlander*, 2000]. Generally, condensation will be thermodynamically favored over homogeneous nucleation, however, under certain conditions, homogeneous nucleation may become an important process in the atmosphere.

[3] Globally, homogeneous nucleation of sulfuric acid is the most important source of new atmospheric particles through homogenous nucleation and formation of thermodynamically stable sulfate clusters [*Kulmala et al.*, 2000]. H_2SO_4 is formed within the atmosphere by oxidation of SO_2 on various pathways and transferred almost completely to the particle phase. Theoretical calculations of homogeneous H_2SO_4 nucleation in the binary H_2SO_4-H_2O system are not consistent with observations in the lower troposphere [*Weber et al.*, 1998]. Ternary nucleation theory in the H_2SO_4-H_2O-NH_3 system yields much better agreement with observations [*Korhonen et al.*, 1999].

[4] In addition to sulfuric acid, a myriad of low-volatile organic compounds exists in the atmosphere, e.g., various oxidation products of reactive hydrocarbons. In forested areas, organic compounds are emitted in large quantities by the vegetation, e.g., isoprene, monoterpenes and sesquiterpenes. More than 40 years ago, *Went* [1960] noted the relevance of biogenically emitted monoterpenes for atmospheric particle formation. Meanwhile, the formation of

[1]Bayreuth Institute of Terrestrial Ecosystem Research (BITÖK), University of Bayreuth, Bayreuth, Germany.
[2]Now at Institute of Landscape Ecology (ILÖK), University of Münster, Münster, Germany.
[3]Institute for Tropospheric Research (IfT), Leipzig, Germany.
[4]Institute for Meteorology and Climate Research (IMK-IFU), Forschungszentrum Karlsruhe, Garmisch-Partenkirchen, Germany.

0148-0227/04/2004JD005346$09.00

low-volatile products from monoterpene oxidation has been demonstrated in many laboratory experiments [e.g., *Hoffmann et al.*, 1997; *Calogirou et al.*, 1999], and also in field experiments [e.g., *Kavouras et al.*, 1998]. Global estimates of secondary particle formation from biogenic precursor gases, though highly variable, are on the order of 18.5 Tg a^{-1} [*Griffin et al.*, 1999a]. It is our goal to contribute to the quantitative understanding of these processes through experimental field campaigns. In the summers of 2001 and 2002, two large field experiments were carried out in the framework of the BEWA2000 joint project of the German atmospheric research program AFO2000 to study emissions of reactive organic compounds from forest stands. Particular attention was given to vertical turbulent fluxes of trace gases and particles as well as interactions between the gas and particle phases.

[5] For a coniferous forest such as the site studied in this work, homogeneous nucleation of H_2SO_4 and formation of thermodynamically stable clusters may be considered as the initial phase of particle formation [*Kulmala et al.*, 2004a]. Even small amounts of NH_3 – such as the typical background of ~1 ppb NH_3 at the observation site – are expected to promote the nucleation tendency of H_2SO_4 [e.g., *Ball et al.*, 1999]. The sulfate clusters are activated through condensation of low-volatile organic compounds leading to nucleation particles of several nm in diameter. For nucleation particles with diameters larger than 3 nm, commercial instruments are available to study the time evolution of the particle concentration and size distribution, and thus the growth dynamics of the particle population.

[6] We present observations of particle formation events and subsequent growth of the nucleation particles above a Norway spruce forest in central Europe. Meteorological and air chemistry conditions during formation events will be compared to "nonevent" situations in order to reveal favorable conditions for homogeneous nucleation. The growth dynamics of the nucleation particles will be quantified and analyzed in detail, and the potential contributions of sulfuric acid and oxidation products of biogenic volatile organic compounds (BVOC) to particle growth will be estimated and evaluated. Finally, we discuss the consequences of the observed dynamics on the emission and deposition fluxes of particles between the vegetation and the atmospheric boundary layer.

2. Methods

[7] During the BEWA field campaigns 2001 and 2002, the turbulent exchange, formation and growth of atmospheric aerosol particles was studied at the "Waldstein" ecosystem research site [*Matzner*, 2004] of the Bayreuth Institute of Terrestrial Ecosystem Research (BITÖK) in the Fichtelgebirge mountains, NE Bavaria, Germany (O. Klemm et al., Experiments on forest/atmosphere exchange: Climatology and fluxes during two summer campaigns in NE Bavaria, submitted to *Atmospheric Environment*, 2004). With an abundance of 93%, Norway spruce is the dominating tree species at this forest site (50°09′N, 11°52′E, 776 m asl).

[8] Particle size distributions were continuously measured using a twin differential mobility particle sizer (TDMPS) [*Birmili et al.*, 1999] with a time resolution of 15–20 min. The setup consisting of two Vienna-type differential mobility analyzers (DMA) for size separation and two condensation particle counters (CPC 3010 and UCPC 3025, TSI Inc., St. Paul, MN, USA) for particle counting covered a size range from 3 to 900 nm diameter in July 2001 and 3–800 nm in July 2002 with 40 size bins, respectively. The mobility distribution was inverted to obtain the particle size distribution applying the bipolar charge distribution, DMA transfer functions, and CPC detection efficiency curves. Ambient air was sampled at 16.7 l min^{-1} through a PM10 inlet mounted at 22 m agl on a 30 m scaffolding tower. The particle sample was introduced into the ground-based DMPS system through 28.5 m of 19.05 mm OD stainless steel tubing at relative humidities below 10%. In order to reconstruct the particle size distribution at ambient relative humidities, an empirical hygroscopic growth model was applied. In this procedure, "wet" particle sizes were related to "dry" particle sizes and ambient relative humidity. Growth factors were determined according to W. Birmili et al. (manuscript in preparation, 2004) using a power law relationship with a sigmoidal function of the particle diameter included in the exponent.

[9] Turbulent particle number fluxes were directly measured employing an eddy covariance system set up 22 m agl at the SE corner of the 30 m tower. The EC system combined a Young Model 81000 ultrasonic anemometer (R. M. Young, Traverse City, MI, USA) and two condensation particle counters (CPC 3760A and UCPC 3025, TSI Inc., St. Paul, MN, USA) with data acquisition operating at 10 Hz. Further details of this system are given elsewhere (A. Held and O. Klemm, Direct measurement of turbulent particle exchange between a coniferous forest and the atmosphere, submitted to *Atmospheric Environment*, 2004, hereinafter referred to as Held and Klemm, submitted manuscript, 2004).

2.1. Particle Dynamics Analysis Tools

[10] After particles have been formed through homogeneous nucleation, these so-called nucleation mode particles grow rapidly through coagulation and condensation processes. Coagulation of nucleation mode particles is highly efficient with larger accumulation mode particles incorporating ultrafine particles and thus removing them from the nucleation mode [*Seinfeld and Pandis*, 1998]. Condensation of low volatile vapors, on the other hand, leads to continuous growth of nucleation mode particles and to a decreasing coagulation rate. The growth rate of newly formed particles through this process was determined by tracking the geometric mean diameter of the nucleation mode. Each individual particle size distribution was parameterized by superposition of up to five lognormal distribution functions representing distinct particle modes using a least squares fitting algorithm [*Birmili et al.*, 2001]. From the three modal parameters describing the lognormal functions, the geometric mean diameter, D_p, in the size range from 3 to 60 nm was used to deduce the particle growth rate during nucleation events. For larger particles, condensation slows down due to diffusional limitation [*Raes et al.*, 2000].

[11] Figure 1a shows a typical nucleation event which exhibits a characteristic "banana-shaped" evolution of the

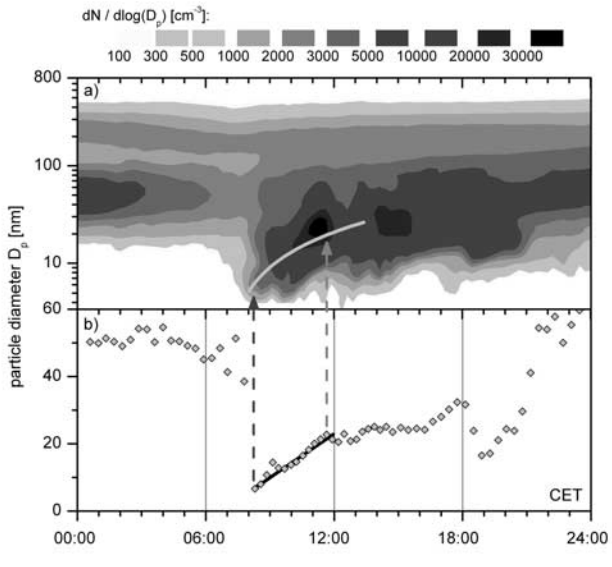

Figure 1. (a) Time evolution of the particle size distribution on 2 August 2001, and geometric mean diameter in the size range 3–60 nm (grey curve). The linear slope appears curved due to logarithmic scaling. (b) Time evolution of the geometric mean diameter in the size range 3–60 nm and linear regression for the time period 08:00–12:00 CET (black line).

particle size distribution (PSD). In order to evaluate growth processes of the newly formed particles from the PSD evolution, stationary conditions of the processes involved have to be assumed. Then, the observed PSD evolution can be described as a quasi-stationary process. For a continuous PSD development as displayed in Figure 1a after 08:15 CET, the stationarity assumption may be considered to be satisfied [*Kulmala et al.*, 1998]. The corresponding geometric mean diameter in the size range from 3 to 60 nm is displayed in the lower panel (Figure 1b). From midnight to 07:00 CET, a stable Aitken mode with a geometric mean diameter around 50 nm can be observed. At 08:15 CET, a steep drop of the geometric mean diameter to 6.7 nm indicates the sudden occurrence of nucleation mode particles. These particles originate from the formation of new particles in the atmosphere through gas-to-particle conversion processes. They continue to grow with a remarkably constant growth rate until noon indicated by the linear slope of the geometric mean diameter. This constant growth rate, dD/dt can be determined from Figure 1b by linear regression. In this example, the slope dD/dt is 4.3 nm h^{-1}. Such a remarkably linear growth has already been observed in several regional nucleation events [*Kulmala et al.*, 2004b]. Also, from theoretical considerations of mass transfer in the kinetic regime, a constant condensational growth rate indicates almost constant concentrations of the condensing vapor(s). *Kulmala et al.* [2001] relate the concentration of the condensing vapor z, c_z, and the radius growth rate, dr/dt, by

$$\frac{dr}{dt} = \frac{M_z \beta_M D_z c_z}{r\rho} \tag{1}$$

with M_z, molar mass of condensing vapor z [g mol^{-1}], β_M, mass transfer correction factor according to *Fuchs and Sutugin* [1970] (dimensionless), D_z, molecular diffusivity of condensing vapor z [m^2 s^{-1}], c_z, concentration of condensing vapor z [mol m^{-3}], r, particle radius [m], and ρ, particle density [g m^{-3}].

[12] The assumption of a constant vapor concentration can also be used to estimate the actual concentration of the condensing vapor from precursor concentrations. In the quasi steady state case, the production and loss rates of the condensing vapor, P and L, are equal, i.e., P = L.

[13] The production rate of the condensing vapor may be estimated if the precursor concentrations and the appropriate reaction constants are available. In cases without direct measurements, precursor concentrations were taken from the one-dimensional canopy chemistry model CACHE (R. Forkel et al., Modelling of trace gas exchange process and gas phase chemistry for a Norway spruce forest with the coupled 1-D Canopy-Chemistry-Emission-Model CACHE, submitted to *Atmospheric Environment*, 2004) using the RACM chemistry mechanism [*Stockwell et al.*, 1997].

[14] For sulfuric acid, the production rate P_{SA} has been estimated by $P_{SA} = k\,[SO_2][OH]$, with k, reaction constant of gas phase oxidation of SO_2 with OH ($8.89 \cdot 10^{-13}$ cm^3 $molec^{-1}$ s^{-1} at 25°C [*Sander et al.*, 2002]), $[SO_2]$, measured concentration of SO_2 [molec cm^{-3}] (SO_2 analyzer Model 8850S, Monitor Labs, USA), [OH], modeled concentration of OH radicals [molec cm^{-3}] (CACHE).

[15] The oxidation of biogenic volatile organic compounds leads to a large variety of low volatile products. In this study at a Norway spruce stand, the oxidation of monoterpenes by O_3, OH, and NO_3 may be considered the most important production pathway of condensable organic vapors with α-pinene being a main component of the isoprenoid emission. Thus the oxidation of α-pinene leading to pinon aldehyde as the main product has been evaluated. In Table 1, the reaction constants of α-pinene with O_3, OH and NO_3 and the approximate fractions of each pathway are summarized.

[16] The total production rate of α-pinene oxidation is the sum of the three pathway production rates. However, only a fraction of the oxidation products is transferred to the particle phase. Therefore the total production rate has to be multiplied with a reasonable aerosol yield factor. In the case of α-pinene oxidation, an aerosol yield of 2% to 15% may be regarded as realistic depending on various factors such as temperature and organic aerosol mass [*Odum et al.*, 1996; *Hoffmann et al.*, 1997; *Griffin et al.*, 1999b; *Kamens*

Table 1. Fraction of O_3, OH, and NO_3 Pathway of α-Pinene Oxidation, and Respective Reaction Constants at 298 K

	O_3	OH	NO_3	Source
Fraction f_x of total oxidation, %	35	45	20	best estimates [cf. *Griffin et al.*, 1999b]
Reaction constant, cm^3 $molec^{-1}$ s^{-1}	$8.66 \cdot 10^{-17}$	$5.37 \cdot 10^{-11}$	$6.16 \cdot 10^{-12}$	*Atkinson* [1994]

et al., 1999]. With regard to organic aerosol mass measurements at the site typically below 5 $\mu g\ m^{-3}$, yields to the lower end of this range may be expected.

[17] The ozone mixing ratio was continuously measured (ML 8810M, Monitor Labs, USA) during the field experiments. Also, atmospheric concentrations and fluxes of α-pinene were measured [*Steinbrecher et al.*, 2004]. Atmospheric concentrations of OH and NO_3 were taken from the CACHE model to estimate the oxidation rate of α-pinene with the above line of reasoning.

[18] The loss rate L of the condensing vapor can be estimated from $L_z = c_z \cdot CondS_z$, the product of the vapor concentration and the condensation sink CondS [*Pirjola et al.*, 1999], a measure of the vapor's tendency to condense on the existing particle surface:

$$CondS_z = 4\pi D_z \sum_j \beta_j r_j N_j \tag{2}$$

with D_z, molecular diffusivity of vapor z [$m^2\ s^{-1}$], β_j, mass transfer correction factor according to *Fuchs and Sutugin* [1970] for size bin j (dimensionless), r_j, particle radius in size bin j [m], and N_j, particle number concentration in size bin j [m^{-3}]. $CondS_z$ may be calculated for any vapor z from the particle size distribution measurements.

[19] Therefore, if the vapor production rate P_z and $CondS_z$ is known, with $P_z = L_z = c_z \cdot CondS_z$, the constant concentration of vapor z can be determined from

$$c_z = \frac{Y \cdot \{f_{O_3} \cdot k_{O_3}[API][O_3] + f_{OH} \cdot k_{OH}[API][OH] + f_{NO_3} \cdot k_{NO_3}[API][NO_3]\}}{CondS_z} \tag{3}$$

with Y, aerosol yield from α-pinene oxidation, f_x, fraction of oxidation pathway with x = O_3, OH, NO_3 (see Table 1), k_x, reaction constants of oxidation with x = O_3, OH, NO_3 (see Table 1), [API]/[O_3]/[OH]/[NO_3], concentrations of α-pinene, ozone, OH and NO_3, respectively, and $CondS_z$, condensation sink (see equation (2)).

2.2. Identification of Nucleation Events

[20] Before analyzing particle dynamics during nucleation events, it is important to select the appropriate tools to identify and evaluate nucleation events from particle size distribution measurements. Formation of thermodynamically stable clusters during homogenous nucleation [*Kulmala et al.*, 2000] leads to ultrafine particles growing to detectable sizes. Thus elevated concentrations of ultrafine particles can be considered as a characteristic indicator for nucleation events. In many cases, the ultrafine particle fraction (e.g., 3–20 nm ⌀) of the total population is an excellent parameter to identify nucleation events.

[21] Another important feature of nucleation events is the characteristic "banana-shaped" evolution of the particle size distribution due to condensation and coagulation processes as displayed in Figure 1a. The "nucleation banana" clearly indicates regional production of particulate matter.

3. Results and Discussion

3.1. Atmospheric Conditions Favoring Nucleation Events

[22] Supersaturated vapors may be transferred to the particulate phase through homogeneous or heterogeneous nucleation. In most cases, condensation is thermodynamically favored over homogeneous nucleation, depending on the degree of supersaturation, the existing particle surface (condensation sink), and meteorological parameters such as shortwave irradiation and atmospheric water content. In Finland, relatively low condensation sinks were observed during nucleation events [e.g., *Nilsson et al.*, 2001]. In contrast, *Birmili and Wiedensohler* [2000] found rather large particle surfaces on nucleation days compared to nonevent days.

[23] In the atmosphere, oxidants such as ozone or the OH radical participate in many chemical reactions leading to condensable vapors. The budgets of these important oxidants are controlled by photochemical mechanisms and thus dependent on shortwave irradiation. *Boy and Kulmala* [2002] found a good correlation of nucleation events and the irradiance in the 320–400 nm wave band (UV-A).

[24] High water vapor concentrations reduce particle formation from monoterpene oxidation products. *Bonn et al.* [2002] proposed competition of water molecules and organic intermediates thus reducing the formation of potentially condensable organic vapors. Also, in field experiments, *Boy and Kulmala* [2002] observed relatively low atmospheric water contents on nucleation days.

[25] Meteorological parameters such as shortwave irradiation, absolute water vapor concentration and ambient temperature can be lumped together to obtain a meteorological nucleation parameter [*Boy and Kulmala*, 2002]. In contrast to the formulation of *Boy and Kulmala* [2002] using the UV-A radiation flux, we included the photolysis frequency of NO_2, $J(NO_2)$, i.e., a measure of the shortwave irradiation from 300 to 380 nm which is a good approximation of the UV-A wave band. Thus a nucleation parameter np was defined as

$$np = \frac{J(NO_2)}{a \cdot T} \tag{4}$$

with $J(NO_2)$, photolysis frequency of NO_2 [s^{-1}], a, absolute humidity at 21 m agl [$g\ m^{-3}$], T, absolute temperature at 21 m agl [K].

[26] Table 2 gives an overview of atmospheric conditions for the observed nucleation events. Within 45 days of DMPS operation during the BEWA campaigns, 13 days were identified indicating nucleation events of varying intensity. Start and end times of the events were determined by tracking the ratio of ultrafine particle concentration (3–20 nm ⌀) and total particle concentration. On event days, the [UFP]/[Total] ratio typically jumped from a constant level below 0.25 over this threshold value (start time), remained on a relatively constant high level and began a continuous decrease after the event (end time). Classification of events is based on a subjective interpretation of the particle size distribution evolution with "+" indicating weak nucleation patterns, "++" an intermediate event type, and "+++" events exhibiting a pronounced banana-shaped development over several hours.

[27] During most nucleation events, S to E winds prevailed. Together with a linear particle growth behavior this indicates regional particle formation and growth processes. Extended forested areas with vegetative and topographic conditions similar to the measuring site are situated to the S

Table 2. Overview of the BEWA Nucleation Events Including the Start and End of Each Event, an Event Classification, the Prevailing Wind Direction, the Maximum Ultrafine Particle Concentration, [UFP] [cm^{-3}], the Ultrafine Particle Fraction of the Total Particle Population, [UFP]/[Total] [−], the Condensation Sink, CondS [10^{-3} s^{-1}], and the Nucleation Parameter, np [10^{-6} m^3 g^{-1} s^{-1} K^{-1}][a]

Date	Start CET	End CET	Quality	Wind Sector	$[UFP]_{max}$	[UFP]/[Total]	CondS	np
5 July 2001	08:00	18:30	+++	N.A.	26759	0.90	5.5	N.A.
12 July 2001	08:00	15:30	++	SW	3959	0.57	3.9	3.82
23 July 2001	08:00	14:00	++	E	21890	0.75	7.7	2.49
27 July 2001	07:00	11:30	++	SE	21993	0.87	6.0	2.23
28 July 2001	07:30	17:00	++	S	8394	0.70	6.3	2.62
2 Aug. 2001	07:30	19:30	+++	SE	8378	0.69	4.6	2.24
nE 2001	07:00	10:00	N.A.	N.A.	1296	0.31	4.0	1.57
3 July 2002	09:30	13:30	+++	S	16772	0.74	6.4	2.64
9 July 2002	07:30	14:00	+	SE	7713	0.53	9.5	2.06
10 July 2002	08:30	12:00	+	SE	17722	0.72	13.9	1.68
12 July 2002	08:30	13:30	+++	SE	30833	0.88	6.0	2.78
27 July 2002	13:30	19:30	++	SE	7162	0.70	5.9	2.01
28 July 2002	09:00	16:00	++	SE	4071	0.40	12.1	2.52
31 July 2002	08:30	12:00	+	SE	8404	0.60	14.9	1.89
nE 2002	08:00	11:00	N.A.	N.A.	835	0.16	9.0	1.51

[a]Given are maximum [UFP] values of the first 3 hours of the event and 3-hour mean values for all other parameters. For comparison, the median parameter values of all nonevent days (nE) are also included for the given 3-hour periods. N.A., not available.

and SE. In particular, relatively uniform conditions of biogenic emission of volatile organic compounds can be expected upwind. Some of these species may be oxidized while traveling from the emission source to the measuring site and these oxidation products may contribute to particle formation. During all nucleation events, maximum particle concentrations in the nucleation mode are found well above 3 nm ∅. A freshly formed particle population, in contrast, should exhibit the highest concentrations at the smallest particle sizes (i.e., 3 nm) because the concentration of larger particles decreases due to self-coagulation and coagulation processes. Therefore we suggest that the measurements are dominated by particles which have already grown for a while, e.g., during their transport to the measuring site.

[28] On July 12, 2001, a nucleation event was observed under SW wind conditions. This event not only exhibited an unusual wind direction, but also the lowest condensation sink and the highest nucleation parameter (equation (4)) of all events. Thus excellent meteorological conditions for homogeneous nucleation and subsequent condensational growth (see Table 3) can be expected. However, low SO_2 mixing ratios (and thus H_2SO_4 concentrations) are the likely reason for very low ultrafine particle concentrations and fractions on this day. In general, the maximum ultrafine particle concentration [UFP] is significantly higher on nucleation days compared to nonevent days with typical ultrafine particle numbers around 1000 cm^{-3}. Also, the UFP fraction during nucleation events is clearly larger than during nonevent situations. A comparison of the condensation sink of nucleation days and nonevent days shows no clear trend. A correlation of nucleation events and low condensation sink values as expected from studies in Finland could not be found in the BEWA campaigns. In fact, rather high condensation sinks during nucleation events are consistent with the results of *Birmili and Wiedensohler* [2000], indicating the abundance of

Table 3. Diameter Growth Rates dD/dt of Observed Particle Formation Events[a]

Date	dD/dt, nm h^{-1}	n	R^2
12 July 2001	5.7	13	0.91
23 July 2001	2.2	33	0.95
27 July 2001	4.3	14	0.96
28 July 2001	2.2	12	0.89
2 Aug. 2001	4.3	13	0.94
3 July 2002	4.4	24	0.93
12 July 2002	3.7	33	0.95
27 July 2002	5.3	16	0.75
28 July 2002	3.2	26	0.93

[a]Here n is the number of data sets used in the linear regression; R^2 is the coefficient of determination.

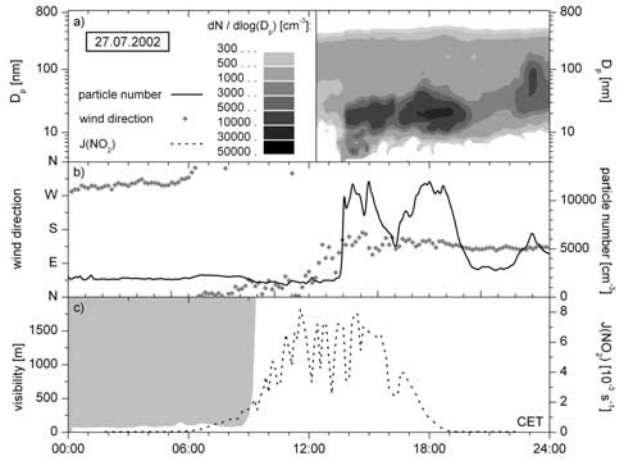

Figure 2. (a) Time evolution of the particle size distribution on 27 July 2002. No data are available for the time before 12:15 CET. (b) Wind direction (grey diamonds) and particle concentration within the forest stand (black line). (c) Visibility (grey shading) and NO_2 photolysis rate, $J(NO_2)$ (dashed line).

Table 4. Typical Values of Precursor Concentrations for H_2SO_4 Production and α-Pinene Oxidation as Used in This Study[a]

Species	Typical Values, ppb	Source
SO_2	<3	MEAS
α-pinene	0.1–1	MEAS/MOD
O_3	40–60	MEAS/MOD
OH	$2 \cdot 10^{-5}$–$1 \cdot 10^{-4}$	MOD
NO_3	$5 \cdot 10^{-5}$–$1.5 \cdot 10^{-4}$	MOD

[a]MEAS indicates measured values, MOD indicates modeled values, and MEAS/MOD indicates use of measured values when available, otherwise modeled values.

condensable vapor. Elevated nucleation parameter values during nucleation events show the applicability of np to identify meteorologically favorable conditions for particle nucleation. These include low relative humidity and high solar irradiation.

[29] Relevant meteorological and air chemistry parameters influencing the nucleation process are shown in Figure 2. During the night and early morning of July 27, 2002, dense fog inhibits nucleation processes (continuous low particle concentrations) and keeps solar irradiation low. Around 09:00 CET, the fog layer dissipates and solar irradiation increases. However, nucleation processes were not observed before 13:30 CET when the wind direction changed from N to SE. This is the key meteorological trigger for the occurrence of nucleation particles, 3 nm < ∅ < 10 nm.

3.2. Observed Particle Diameter Growth Rates

[30] During the BEWA field campaigns, 10 nucleation events classified as "++" or "+++" (see Table 2) were observed. For nine of these events, particle growth rates could be evaluated through linear regression analysis of the geometric mean diameter of the ultrafine particle fraction as displayed in Figure 1b. The linear growth behavior during nucleation events is evident from the high correlation coefficients of the linear regression model.

[31] Table 3 shows the observed particle diameter growth rates, dD/dt, ranging from 2.2 to 5.7 nm h^{-1}. The corresponding coefficients of determination, R^2, range from 0.75 to 0.96 using 12 to 33 data points for the linear regression analysis. In seven cases, R^2 is larger than 0.90 indicating the excellent applicability of the linear model.

3.3. Evaluation of H_2SO_4 and Organic Vapor Contributions to Particle Growth

[32] Using equation (1), the observed particle growth rates of freshly nucleated particles may be related to theoretically expected concentrations of condensing vapors, and these concentrations were compared to ambient concentrations of condensable vapors. For sulfuric acid, a molecular mass M (H_2SO_4) of 98 g mol^{-1} and a molecular diffusivity D (H_2SO_4) of $0.752 \cdot 10^{-5}$ m^2 s^{-1} was used. With pinon aldehyde as the main product of the α-pinene oxidation, the condensable organic vapor (COV) was assigned a molecular mass M (COV) of 168 g mol^{-1}. The molecular diffusivity of the condensable organic vapor, D (COV), was approximated by use of Graham's law [*Thibodeaux*, 1996]. Particle density ρ was set to 1.3 g cm^{-3} taking into account the higher densities of inorganic compounds and the lower densities of organic compounds and water. Using these parameters and the precursor species as displayed in Table 4, ambient concentrations of H_2SO_4 and the α-pinene oxidation product were estimated as described in the "Analysis Tools" section. Then, the corresponding growth rates were calculated. For the comparison of theoretical and observed growth rates in Table 5, the condensing fraction of the organic vapor, i.e., the aerosol mass yield from α-pinene oxidation, was assumed to be 5% as a conservative estimate.

[33] Apparently, the ambient H_2SO_4 concentrations are too low to explain the observed particle growth behavior. On most days, less than 10% of the observed growth rates can be explained by condensation of H_2SO_4. Taking into account the cocondensation of water vapor during H_2SO_4 condensation to maintain a molar ratio of H_2SO_4 and H_2O consistent with the gas phase ratio [*Clement and Ford*, 1999], still only a small fraction of the condensational growth may be explained through this process. However, condensation of the α-pinene oxidation product contributes significantly to the observed particle growth. Even under the conservative assumption of a 5% mass yield, a large fraction of the observed growth can be explained.

[34] The exact contribution of condensable organic vapors to particle growth cannot be calculated due to the

Table 5. Estimated Atmospheric Concentrations of H_2SO_4 and Condensable Organic Vapors From the Oxidation of α-Pinene With a 5% Aerosol Mass Yield (COV5), Theoretical Particle Growth Rates, Observed Particle Growth Rates, and the Explained Fraction of the Observed Particle Growth[a]

	Concentration, molec cm^{-3}		dD/dt, nm h^{-1}, Due to		dD/dt, nm h^{-1}	Explained Fraction,%							
Date	H_2SO_4	COV5	H_2SO_4	COV5	Observed	H_2SO_4	COV5	T, °C	rH, %	I, W m^{-2}	[OH], molec cm^{-3}	[NO_3], molec cm^{-3}	[O_3], ppb
12 July 2001	$7.3 \cdot 10^5$	$1.3 \cdot 10^7$	0.04	0.95	5.7	1	17	14.6	57.8	719	$1.3 \cdot 10^6$	$2.0 \cdot 10^6$	37.5
23 July 2001	$2.2 \cdot 10^6$	$1.6 \cdot 10^7$	0.13	1.16	2.2	6	53	21.8	49.1	417	$4.8 \cdot 10^5$	$2.6 \cdot 10^6$	48.1
27 July 2001	$7.3 \cdot 10^6$	$1.3 \cdot 10^7$	0.41	0.92	4.3	10	21	21.8	49.3	459	$8.9 \cdot 10^5$	$2.8 \cdot 10^6$	56.3
28 July 2001	$6.6 \cdot 10^6$	$1.2 \cdot 10^7$	0.38	0.91	2.2	17	41	21.7	52.2	616	$8.0 \cdot 10^5$	$3.1 \cdot 10^6$	58.0
2 Aug. 2001	$3.9 \cdot 10^6$	$1.2 \cdot 10^7$	0.22	0.89	4.3	5	21	17.6	65.4	505	$6.1 \cdot 10^5$	$3.4 \cdot 10^6$	37.8
3 July 2002	$1.2 \cdot 10^6$	$8.9 \cdot 10^6$	0.07	0.65	4.4	2	15	18.8	55.3	710	$1.3 \cdot 10^6$	$2.0 \cdot 10^6$	44.1
12 July 2002	$8.0 \cdot 10^5$	$1.6 \cdot 10^7$	0.05	1.21	3.7	1	33	19.8	45.7	666	$9.6 \cdot 10^5$	$1.7 \cdot 10^6$	52.6
28 July 2002	$3.2 \cdot 10^6$	$1.4 \cdot 10^7$	0.18	1.06	3.2	6	33	22.2	46.2	814	$1.7 \cdot 10^6$	$1.8 \cdot 10^6$	58.0

[a]Additional parameters include temperature (T), relative humidity (rH), global irradiance (I), the concentrations of OH, NO_3, and the O_3 mixing ratio, respectively.

Table 6. Theoretical Mass Yield of α-Pinene Oxidation Needed to Fully Explain the Observed Particle Growth Through Condensation of H_2SO_4 and α-Pinene Oxidation Products

Date	Theoretical Mass Yield
12 July 2001	30
23 July 2001	9
27 July 2001	21
28 July 2001	10
2 Aug. 2001	23
3 July 2002	33
12 July 2002	15
28 July 2002	14

unknown aerosol mass yield of the various oxidation reactions of volatile organic compounds. However, with the above calculations it is possible to theoretically estimate the mass yield needed to fully explain the observed growth dynamics by cocondensation of H_2SO_4 and α-pinene oxidation products. After subtracting the H_2SO_4 contribution from the observed growth, the theoretical aerosol mass yield of the oxidation of α-pinene that is sufficient to yield the remaining condensational growth can be calculated from equations (1) and (3). Table 6 gives the range of theoretically needed mass yields for eight different events.

[35] With a plausible range of α-pinene oxidation mass yields up to 15%, it is possible to fully explain the observed particle growth by cocondensation of H_2SO_4 and α-pinene oxidation products on half of the studied days. On all other days, additional condensable vapors have to be considered.

3.4. Discussion

[36] During the BEWA field campaigns, indications of particle formation were found on 13 of 45 measuring days. Thus particle formation may be considered a frequent process at the "Waldstein" forest site in summer consistent with studies at other sites [e.g., *Birmili et al.*, 2003; *Mäkelä et al.*, 2000]. Wind direction is a crucial meteorological parameter for observations of particle formation. The prevailing winds from S and E during formation events indicate an important impact of the extensive coniferous forests situated in the fetch area upwind of the site. Other meteorological parameters showed a consistent trend favoring formation events during dry conditions with intense radiation. However, no predictive capability could be derived from these parameters. Also, no clear correlation of nucleation events and low condensation sink values was found during BEWA.

[37] Remarkably constant growth rates of nucleation particles were observed and quantified objectively by means of linear regression analysis. This growth behavior indicates regional formation events occurring over a wide area [*Kulmala et al.*, 2004b], in this study over wide-stretched areas of coniferous forest. The observed particle growth rates ranging from 2.2 to 5.7 nm h^{-1} are consistent with typical growth rates found at different sites as summarized in Table 7.

[38] From Table 7 a range of diameter growth rates from 1 to 10 nm h^{-1} may be assumed typical for most rural and urban areas. In contrast, growth rates up to 180 nm h^{-1} have been observed in coastal areas, while small growth rates around 0.1 nm h^{-1} have been found in remote polar regions.

[39] The quantification of the contribution of different species to condensational particle growth is limited by uncertainties of the H_2SO_4 and organic vapor concentration estimates. Nevertheless, at least a semiquantitative comparison of the vapor contributions is feasible with the presented procedure. From the calculations it is evident that H_2SO_4 is not sufficient to maintain the observed particle growth. In contrast, even with a conservative estimate for the aerosol yield the condensation of α-pinene oxidation products explains a considerable fraction of the particle growth rates. The relevance of organic vapor condensation is also supported by the fact that formation events were almost exclusively observed when the fetch was dominated by coniferous forests emitting reactive organic compounds. α-pinene oxidation products such as pinon aldehyde, pinonic acid, pinic acid, norpinic acid, and many other BVOC products were identified in the particle phase through chemical analysis of impactor samples (T. Gnauk et al., manuscript in preparation, 2004). Given this result and the calculated estimates of their particle formation potential, we conclude that biogenic emissions of reactive organic compounds play a vital role in the process of particle growth at the site of this study.

[40] The particle formation process is not obvious in direct eddy covariance measurements of vertical particle number fluxes (Held and Klemm, submitted manuscript, 2004). Turbulent particle fluxes from the atmosphere to the vegetation dominate at the site, and during particle formation events, the strongest particle deposition fluxes were observed. For example, on August 2, 2001, nucleation particles occurred around 07:30 CET and continued to grow to Aitken mode sizes over the day (Figure 3a). The sudden occurrence of nucleation particles coincides with the onset

Table 7. Experimental Particle Growth Rates at Different Sites

dD/dt, nm h^{-1}	Site	Description	Source
0.13	South Pole	remote	*Park et al.* [2004][a]
1.9–3.8	Värriö	sub-Arctic, remote	*Pirjola et al.* [1998][a]
3–4.5	Jungfraujoch	remote	*Weingartner et al.* [1999]
2–3	Hyytiälä	rural, coniferous forest	*Kulmala et al.* [2001]
4.1	Melpitz	rural	*Birmili and Wiedensohler* [2000]
0.5–8.4	Hohenpeißenberg	rural	*Birmili et al.* [2003]
4–5	Pittsburgh	urban	*Stanier et al.* [2002]
2–5	Macquarie Island	marine	*Weber et al.* [1998]
15–180	Mace Head	coastal	*O'Dowd et al.* [2002]
2.2–5.7	Waldstein	rural, coniferous forest	this study

[a]Cited from *Kulmala et al.* [2004b].

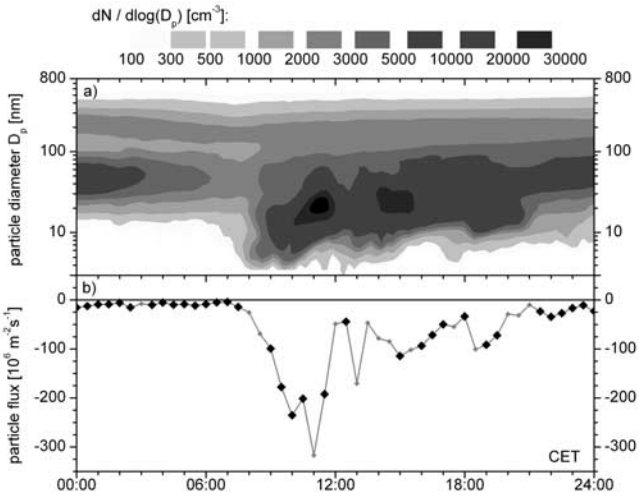

Figure 3. (a) Time evolution of the particle size distribution on 2 August 2001. (b) Turbulent particle number flux on 2 August 2001. Black diamonds indicate high-quality data; data displayed in gray failed one or more quality tests.

of particle deposition reaching a maximum just before noon (Figure 3b).

[41] These findings imply that if particles have been formed within the forest stand, i.e., below the measuring height of the eddy covariance system, they must have been emitted from the forest as particles smaller than the minimum particle diameter of 3 nm detectable by the ultrafine condensation particle counter. Another possibility is the emission of organic vapors from the forest stand contributing to the growth of TSC and particles above the forest stand. In both cases, nucleation particles are formed and after continued growth, particles larger than 3 nm may be detected by the flux system as depositing particles. This supports our findings that BVOC emissions from the forest lead to particle growth to detectable sizes on the time scale of hours. Theoretical particle deposition models [e.g., *Slinn*, 1982] predict high deposition velocities for nucleation particles. These high deposition velocities and the large number of nucleation particles during particle formation events are reflected in strong particle deposition events as displayed in Figure 3b.

4. Conclusions

[42] Particle formation events have been observed in 22% of the BEWA field experiment days indicating that nucleation and subsequent growth of particles may be considered a frequent phenomenon in the atmospheric boundary layer. Also, the particle growth dynamics are consistent with earlier studies supporting the assumption of a general nucleation mechanism which may be modeled to gain deeper insight into particle nucleation and growth dynamics [e.g., *Lehtinen and Kulmala*, 2003].

[43] Several aspects of the BEWA field experiments revealed the relevance of BVOC emissions for particle formation in the atmosphere: (1) During particle formation events, S to E winds prevailed with extended areas of coniferous forest (and potentially high BVOC emissions) upwind of the measuring site, where particle formation and growth processes could occur on the time scale of hours. (2) A comparison of theoretical and observed growth rates showed that condensation of organic vapors (with precursors being emitted from the forest) is very likely to maintain a large fraction of the observed particle growth. (3) Analysis of the particle chemical composition found oxidation products of BVOC such as α-pinene in the particle phase. These indications leave no doubt that particle mass was formed in the atmosphere from biogenic emissions of organic compounds.

[44] However, the presence of the forest stand also enhances particle deposition at the site, and thus particle removal from the atmosphere. Increased particle deposition is due to increased surface roughness above forest areas as compared to, e.g., grassland, and also effective removal through impaction and interception of particles on the needle surfaces.

[45] In summary, the eddy covariance particle flux measurements yield net deposition of particles making the forest a sink of particle number, while the evolution of the particle size distribution indicates particle formation and growth making the forest a source of particulate matter. Thus the net effect of the forest stand on particle mass remains unclear in this study. To further investigate this question, size-resolved measurements of particle number and mass fluxes are needed. Therefore innovative combinations of instruments and methods with the potential to derive chemical composition fluxes of the particulate phase [e.g., *Held et al.*, 2003] are major tasks for future atmospheric boundary layer research.

[46] **Acknowledgments.** This study was funded by the German federal ministry of education and research (BMBF) through grants PT BEO 51–0339476 D (BITÖK) and PT UKF 07ATF25 (BEWA). The authors appreciate the help of J. Gerchau and G. Müller during data collection and the support of the BEWA community.

References

Atkinson, R. (1994), *Gas-Phase Tropospheric Chemistry of Organic Compounds*, 216 pp., Am. Inst. of Phys., College Park, Md.

Ball, S. M., D. R. Hanson, F. L. Eisele, and P. H. McMurry (1999), Laboratory studies of particle nucleation: Initial results for H_2SO_4, H_2O, and NH_3 vapors, *J. Geophys. Res.*, *104*, 23,709–23,718.

Birmili, W., and A. Wiedensohler (2000), New particle formation in the continental boundary layer: Meteorological and gas phase parameter influence, *Geophys. Res. Lett.*, *27*, 3325–3328.

Birmili, W., F. Stratmann, and A. Wiedensohler (1999), Design of a DMA-based size spectrometer for a large particle size range and stable operation, *J. Aerosol Sci.*, *30*, 549–553.

Birmili, W., A. Wiedensohler, J. Heintzenberg, and K. Lehmann (2001), Atmospheric particle number size distribution in central Europe: Statistical relations to air masses and meteorology, *J. Geophys. Res.*, *106*, 32,005–32,018.

Birmili, W., H. Berresheim, C. Plass-Dülmer, T. Elste, S. Gilge, A. Wiedensohler, and U. Uhrner (2003), The Hohenpeissenberg aerosol formation experiment (HAFEX): A long-term study including size-resolved aerosol, H_2SO_4, OH, and monoterpenes measurements, *Atmos. Chem. Phys.*, *3*, 361–376.

Bonn, B., G. Schuster, and G. K. Moortgat (2002), Influence of water vapor on the process of new particle formation during monoterpene ozonolysis, *J. Phys. Chem. A*, *106*, 2869–2881.

Boy, M., and M. Kulmala (2002), Nucleation events in the continental boundary layer: Influence of physical and meteorological parameters, *Atmos. Chem. Phys.*, *2*, 1–16.

Calogirou, A., B. R. Larsen, and D. Kotzias (1999), Gas-phase terpene oxidation products: A review, *Atmos. Environ.*, *33*, 1423–1439.

Clement, C. F., and I. J. Ford (1999), Gas-to-particle conversion in the atmosphere: II. Analytical models of nucleation bursts, *Atmos. Environ.*, *33*, 489–499.

Friedlander, S. (2000), *Smoke, Dust, and Haze: Fundamentals of Aerosol Dynamics*, 480 pp., Oxford Univ. Press, New York.

Fuchs, N. A., and A. G. Sutugin (1970), *High Dispersed Aerosols*, 105 pp., Ann Arbor Sci., Ann Arbor, Mich.

Griffin, R. J., D. R. Cocker, J. H. Seinfeld, and D. Dabdub (1999a), Estimate of global atmospheric organic aerosol from oxidation of biogenic hydrocarbons, *Geophys. Res. Lett.*, *26*, 2721–2724.

Griffin, R. J., D. R. Cocker, R. C. Flagan, and J. H. Seinfeld (1999b), Organic aerosol formation from the oxidation of biogenic hydrocarbons, *J. Geophys. Res.*, *104*, 3555–3567.

Held, A., K. P. Hinz, A. Trimborn, B. Spengler, and O. Klemm (2003), Towards direct measurement of turbulent vertical fluxes of compounds in atmospheric aerosol particles, *Geophys. Res. Lett.*, *30*(19), 2016, doi:10.1029/2003GL017854.

Hoffmann, T., J. R. Odum, F. Bowman, D. Collins, D. Klockow, R. C. Flagan, and J. H. Seinfeld (1997), Formation of organic aerosols from the oxidation of biogenic hydrocarbons, *J. Atmos. Chem.*, *26*, 189–222.

Kamens, R., M. Jang, C. J. Chien, and K. Leach (1999), Aerosol formation from the reaction of (-pinene and ozone using a gas-phase kinetics-aerosol partitioning model, *Environ. Sci. Technol.*, *33*, 1430–1438.

Kavouras, I. G., N. Mihalopoulos, and E. G. Stephanou (1998), Formation of atmospheric particles from organic acids produced by forests, *Nature*, *395*, 683–686.

Korhonen, P., M. Kulmala, A. Laaksonen, Y. Viisanen, R. McGraw, and J. H. Seinfeld (1999), Ternary nucleation of H_2SO_4, NH_3, and H_2O in the atmosphere, *J. Geophys Res.*, *104*, 26,349–26,353.

Kulmala, M., A. Toivonen, J. M. Mäkelä, and A. Laaksonen (1998), Analysis of the growth of nucleation mode particles observed in boreal forest, *Tellus, Ser. B.*, *50*, 449–462.

Kulmala, M., L. Pirjola, and J. M. Mäkelä (2000), Stable sulphate clusters as a source of new atmospheric particles, *Nature*, *404*, 66–69.

Kulmala, M., M. Dal Maso, J. M. Mäkelä, L. Pirjola, M. Väkevä, P. Aalto, P. Miikkulainen, K. Hämeri, and C. D. O'Dowd (2001), On the formation, growth and composition of nucleation mode particles, *Tellus, Ser. B*, *53*, 479–490.

Kulmala, M., V. M. Kerminen, T. Anttila, A. Laaksonen, and C. D. O'Dowd (2004a), Organic aerosol formation via sulphate cluster activation, *J. Geophys. Res.*, *109*, D04205, doi:10.1029/2003JD003961.

Kulmala, M., H. Vehkamäki, T. Petäjä, M. Dal Maso, A. Lauri, V. M. Kerminen, W. Birmili, and P. H. McMurry (2004b), Formation and growth rates of ultrafine atmospheric particles: A review of observations, *J. Aerosol Sci.*, *35*, 143–176.

Lehtinen, K. E. J., and M. Kulmala (2003), A model for particle formation and growth in the atmosphere with molecular resolution in size, *Atmos. Chem. Phys.*, *3*, 251–257.

Mäkelä, J. M., I. K. Koponen, P. Aalto, and M. Kulmala (2000), One-year data of submicron size modes of tropospheric background aerosol in southern Finland, *J. Aerosol Sci.*, *31*, 595–611.

Matzner, E. (Ed.) (2004), *Biogeochemistry of Forested Catchments in a Changing Environment*, *Ecol. Stud.*, vol. 172, 498 pp., Springer-Verlag, New York.

Nilsson, E. D., Ü. Rannik, M. Kulmala, G. Buzorius, and C. D. O'Dowd (2001), Effects of continental boundary layer evolution, convection, turbulence and entrainment on aerosol formation, *Tellus, Ser. B*, *53*, 441–461.

O'Dowd, C. D., et al. (2002), A dedicated study of new particle formation and fate in the coastal environment (PARFORCE): Overview of objectives and achievements, *J. Geophys. Res.*, *107*(D19), 8108, doi:10.1029/2001JD000555.

Odum, J. R., T. Hoffmann, F. Bowman, D. Collins, R. C. Flagan, and J. H. Seinfeld (1996), Gas/particle partitioning and secondary organic aerosol yields, *Environ. Sci. Technol.*, *30*, 2580–2585.

Park, J., H. Sakurai, K. Vollmers, and P. H. McMurry (2004), Aerosol size distributions measured at the south pole during ISCAT, *Atmos. Environ.*, in press.

Pirjola, L., A. Laaksonen, P. Aalto, and M. Kulmala (1998), Sulfate aerosol formation in the arctic boundary layer, *J. Geophys. Res.*, *103*, 8309–8321.

Pirjola, L., M. Kulmala, M. Wilck, A. Bischoff, F. Stratmann, and E. Otto (1999), Formation of sulphuric acid aerosols and cloud condensation nuclei: An expression for significant nucleation and model comparison, *J. Aerosol Sci.*, *30*, 1079–1094.

Raes, F., R. Van Dingenen, E. Vignati, J. Wilson, J. P. Putaud, J. H. Seinfeld, and P. Adams (2000), Formation and cycling of aerosols in the global troposphere, *Atmos. Environ.*, *34*, 4215–4240.

Sander, S. P., et al. (2002), Chemical kinetics and photochemical data for use in atmospheric studies, Evaluation 14, *JPL Publ., 02-25*, 310 pp.

Seinfeld, J. H., and S. N. Pandis (1998), *Atmospheric Chemistry and Physics: From Air Pollution to Climate Change*, 1326 pp., John Wiley, Hoboken, N. J.

Slinn, W. G. N. (1982), Predictions for particle deposition to vegetative surfaces, *Atmos. Environ.*, *16*, 1785–1794.

Stanier, C. O., A. Y. Khlystov, and S. N. Pandis (2002) Investigation of nucleation bursts during the Pittsburgh air quality study, paper presented at Sixth International Aerosol Conference, Chin. Assoc. for Aerosol Res. in Taiwan, Taipei.

Steinbrecher, R., B. Rappenglück, A. Hansel, M. Graus, O. Klemm, A. Held, A. Wiedensohler, and A. Nowak (2004), Vegetation-atmospheric interactions: The emissions of biogenic volatile organic compounds (BVOC) and their relevance to atmospheric particle dynamics, in *Biogeochemistry of Forested Catchments in a Changing Environment: A Case Study in NE-Bavaria, Germany*, *Ecol. Stud.,* vol. 172, edited by E. Matzner, pp. 215–232, Springer-Verlag, New York.

Stockwell, W. R., F. Kirchner, M. Kuhn, and S. Seefeld (1997), A new mechanism for regional atmospheric chemistry modelling, *J. Geophys. Res.*, *102*, 25,847–25,879.

Thibodeaux, L. J. (1996), *Environmental Chemodynamics*, 593 pp., John Wiley, Hoboken, N. J.

Weber, R. J., P. H. McMurry, L. Mauldin, D. J. Tanner, F. L. Eisele, F. J. Brechtel, S. M. Kreidenweis, G. L. Kok, R. D. Schillawski, and D. Baumgardner (1998), A study of new particle formation and growth involving biogenic and trace gas species measured during ACE 1, *J. Geophys. Res.*, *103*, 16,385–16,396.

Weingartner, E., S. Nyeki, and U. Baltensperger (1999), Seasonal and diurnal variation of aerosol size distributions ($10 < D < 750$ nm) at a high-alpine site (Jungfraujoch 3580 m asl), *J. Geophys. Res.*, *104*, 26,809–26,820.

Went, F. W. (1960), Blue hazes in the atmosphere, *Nature*, *187*, 641–643.

Wexler, A. S., and J. H. Seinfeld (1990), The distribution of ammonium salts among a size and composition dispersed aerosol, *Atmos. Environ., Part A*, *24*, 1231–1246.

W. Birmili, A. Nowak, and A. Wiedensohler, Institute for Tropospheric Research (IfT), 04318 Leipzig, Germany.

R. Forkel, Institute for Meteorology and Climate Research (IMK-IFU), Forschungszentrum Karlsruhe, D-82467 Garmisch-Partenkirchen, Germany.

A. Held and O. Klemm, Institute of Landscape Ecology (ILÖK), University of Münster, 48149 Münster, Germany. (andreas.held@uni-muenster.de)